APPLICATION NOTE 2

2020

The application note of the Marie Curie Skłodowska European Training Network

Bimodal AFM

INTRODUCTION

The Atomic Force Microscope bases its working mechanism on the force sensed by a probe, usually a tip attached to a cantilever, with a defined sample [1]. This force can be of different nature, i.e. long and short range. The mechanical characteristics of a material can be derived analyzing the mechanical contact between the tip and the sample [2]. These properties at the nanoscale have important consequences on the behaviour of different kind of materials. Examples are found in material science, such as for polymers, where the spatial diversities of their properties or in the case of multicomponent systems determines a complex bulk mechanical behaviour. Therefore, being able to connect the nanoscale morphology with the mechanical properties provides a way to link nanoscale structures to intrinsic properties of the material. Furthermore, in biology, the viscoelastic behaviour of cells has been linked to their life cycle and health condition.

Dynamic AFM techniques are currently leading methods when it comes to combine high resolution and properties mapping at the nanoscale [3]. They are based on the excitation, usually through a piezo, of the cantilever in one of its eigenmodes. It is possible to recognize four basic dynamic AFM technique: amplitude modulation (AM) or tapping mode, frequency modulation (FM), phase modulation (PM), where a single cantilever's mode is excited, and multifrequency AFM, where multiple modes are driven simultaneously. Bimodal AFM is a multifrequency technique and consists in the excitation of two of its modes [4,5]. Currently, AM-FM, AM-AM and FM-FM are the mostly used bimodal set-up [6]. Since bimodal AFM works in a similar way than tapping mode it is simple and straightforward to use. Moreover, it is possible to run it in a fast way, even reaching the high speed limit of high speed AFM microscopes, it has the advantage of applying gentle forces (indentation of a few nm) and of easily achieving high spatial resolution (in the angstrom regime).

BIMODAL AFM WORKING PRINCIPLES

Usually, in a bimodal configuration, the first two cantilever's flexural modes are excited, with the first mode having an excitation amplitude at least 10 times higher than the one of the second mode. This is required in the case of viscoelastic mapping [7]. When the purpose of the experiment is of high resolution imaging only, this rule doesn't have to be followed, and different combination of exciting amplitudes were tried in order to optimize the quality of the resulting image [8].

Let's consider the AM-FM configuration: the first resonance is operated in AM, the free amplitude and phase (A_{01} and φ_1) are fixed at a chosen frequency, ω_1, and a lock-in amplifier measures their changes. The AM controller performs the main feedback mechanism, keeping constant the amplitude, at a certain set-point A_1, by tuning the cantilever's vertical position. In a mechanical mapping experiment, φ_1 must be kept below 90°, i.e. operated in the repulsive regime. At the same time, a FM controller works on the second eigenmode. A phase-lock-loop regulates the excitation frequency ω_2 by keeping the phase at 90°, and a feedback tunes the power in order to maintain the amplitude constant, A_2. In high Q environment, the phase of the first mode contains dissipative information while the frequency of the second mode provides a qualitative measure of the sample's stiffness.

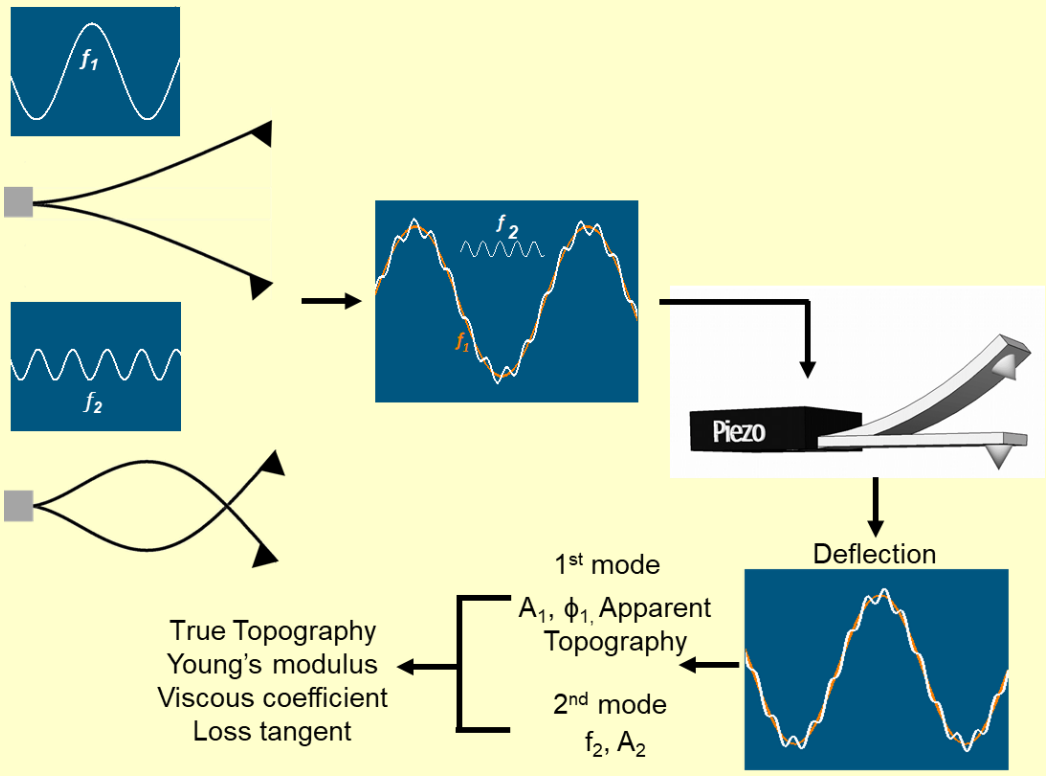

Figure 1. Bimodal AM-FM scheme. Two excitation signals are combined in order to excite the cantilever in its first and second mode. By scanning the surface, the deflection signal is recorded and processed to finally obtain the bimodal observables. From those observables, a theoretical framework is applied and the nanomechanical parameters are reconstructed.

ELASTIC AND VISCOELASTIC MAPPING

The theory that translates the bimodal observables into viscoelastic properties is based on the virial and energy dissipation theorem [3]. Assuming a spherical shape for the tip and a force of the Kelvin-Voigt type, which contains the elastic (Young's modulus, E_{eff}) and viscous component (viscous coefficient of compressibility, η_{com}) it was demonstrated that [9]

$$E_{eff} = \sqrt{\frac{8A_1}{R}\frac{V_2^2}{V_1}\frac{A_1}{A_2^4}} \tag{1}$$

$$\eta_{com} = (2\pi\omega_1)^{-1} E_{eff}\frac{E_{dis1}}{V_1} \tag{2}$$

where V_1 and V_2 are the virial of the first and second mode, E_{dis1} is the energy dissipation of the first mode and R is the tip's radius. Finally, it is possible to link the E_{dis1}/V_1 to the definition of the loss tangent ($\tan\rho$) and to the characteristic time of the K-V model, i.e. the retardation time (τ)

$$\tan\rho = \omega_1\frac{\eta_{com}}{E_{eff}} = \omega_1\tau \tag{3}$$

Figure 2. Bimodal viscoelastic reconstruction of a PS-b-PMMA (polystyrene-b- poly(methyl methacrylate) sample. a, Young's modulus map; b, viscous coefficient of compressibility map; c, retardation time map, which is directly linked to the loss tangent value. Adapted from [9].

TRUE TOPOGRAPHY RECONSTRUCTION AND TIP'S RADIUS

The AFM is widely used to map properties of soft materials, such as polymers and biological samples. Since their surface is highly deformable we cannot consider the topographical image coming directly from the first mode feedback as real (apparent topography, h_{app}). Usually in tapping mode AFM this effect is ignored. Nonetheless, in bimodal AFM there is the possibility to reconstruct the true topography (h_{true}) of the sample taking into account the applied deformation (δ_{max})

$$\delta_{max} = \left(\frac{A_2^2}{A_1}\right)\left(\frac{V_1}{V_2}\right) \quad (4)$$

$$h_{true} = h_{app} + \delta_{max} \quad (5)$$

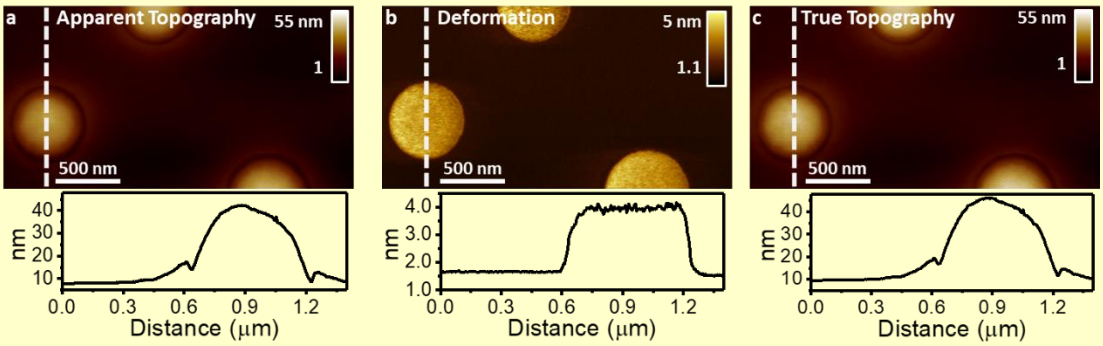

Figure 3. True topography reconstruction of a PS-LDPE (polystyrene-Low density polyethylene) blend. a, Apparent topography map; b, Deformation map; c, True topography map. Below each figures the cross sections taken along the white dashed lines are shown. Unpublished data.

Another issue to face is the determination of the tip's radius, which is needed to determine the nanomechanical properties of the sample. The first consideration that must be done is that for a paraboloid indenter as in our case $R \geq \delta_{max}$. Two ways of determining R are proposed: the first is based on the resolution achieved in the sample, determining the radius of curvature through a fit in the point of maximum resolution; the second consists in performing a bimodal nanomechanical characterization on a sample with known viscoelastic characteristics, tuning the radius accordingly.

BIMODAL AFM NEW PERSPECTIVES

The fact that bimodal AM-FM is based on the dynamic mode AFM gives opportunities for further advances. This feature makes bimodal AFM a natural partner to high-speed AFM which is based on the same working mechanism [10]. This is shown in Figure 4 where the same PS-b-PMMA block copolymer of Figure 2 (170 s per frame) is mapped at high-speed (5 s per frame). It is possible to notice that the bimodal observable that links to the nanomechanical properties (2nd mode frequency) is resolved with high spatial resolution as it would happen in the case of conventional bimodal AFM. This opens up possibilities in the field of polymer science and especially of biology where mechanical properties play a role in cell's life condition or proteins' functions [11].

REFERENCES

1. G. Binnig, C. F. Quate, and C. Gerber, Phys. Rev. Lett. **56**, 930 (1986)
2. R. Garcia, Chem. Soc. Rev. **49**, 5850 (2020)
3. R. Garcia, *Amplitude Modulation Atomic Force Microscopy* (Wiley-VCH Verlag GmbH & Co. KGaA, Weinheim, Germany, 2010)
4. T. R. Rodríguez and R. Garcia, Appl. Phys. Lett. **84**, 449 (2004)
5. A. Labuda, M. Kocun, W. Meinhold, D. Walters, and R. Proksch, Beilstein J. Nanotechnol. **7**, 970 (2016)
6. R. Garcia and R. Proksch, Eur. Polym. J. **49**, 1897 (2013)
7. C. A. Amo, A. P. Perrino, A. F. Payam, and R. Garcia, ACS Nano **11**, 8650 (2017)
8. H. Ooe, D. Kirpal, D. S. Wastl, A. J. Weymouth, T. Arai, and F. J. Giessibl, Appl. Phys. Lett. **109**, 141603 (2016)
9. S. Benaglia, C. A. Amo, and R. Garcia, Nanoscale **11**, 15289 (2019)
10. T. Ando, N. Kodera, E. Takai, D. Maruyama, K. Saito, and A. Toda, Proc. Natl. Acad. Sci. **98**, 12468 (2001)
11. Y.-C. Lin, Y. R. Guo, A. Miyagi, J. Levring, R. MacKinnon, and S. Scheuring, Nature (2019)